Received September 1998
Revised April 1999
Accepted May 1999

Predictions of swirling flow in sudden-expansion dump combustor with flameholder side-inlet using two-step combustion model

Shu-Hao Chuang
Department of Mechanical Engineering, National Chung-Hsing University, Taichung, Taiwan, Republic of China
Chih-Sheng Yang
Far East Engineering and Business College, Tainan, Taiwan, Republic of China, and
Nein-Jou Wu
Industrial Technology Research Institute, Center of Aeronautics and Astronautics, Hsinchu, Taiwan, Republic of China

Keywords *Flow, Combustion*

Abstract *The swirling flow of sudden-expansion dump combustor with central V-gutter flameholder and six side-inlets is studied by employing the SIMPLE-C algorithm and Jones-Launder k-ε two-equation turbulent model. Both combustion models of one-step with infinite chemical reaction rate and two-step with finite chemical reaction rate of eddy-breakup (EBU) model are used to solve the present problem. The results agreed well with available prediction data in terms of axial-velocity and total pressure coefficient along combustor centerline. The flowfield structure of combustor considered is strongly affected by swirling, flameholder and side-inlet flow. For the fixed strength of swirling, the length of central recirculation zone is decreased when the angle of V-gutter is increased. The outlet velocity of combustor in reacting flow is higher than that in cold flow because the released heat of combustion causes the decrease of density throughout the combustor flowfield. The distribution of mass fraction of various species in reacting process depends on the mixing effect, chemical kinetic and the geometric configuration of combustor.*

Nomenclature

A_i = surface area of cell
A/F = air-fuel ratio
a_i = coefficient
BR = blockage ratio
C_p = specific heat at constant pressure
C_{pt} = total pressure coefficient
D = radius of the combustor
d = radius of the combustor inlet
DR = dump ratio
f = mixture mass-fraction
Δh_f^o = heat of reaction per unit mass of fuel
H = total enthalpy
k = turbulence kinetic energy
p = static pressure
Re = Reynolds number
S_ν = source term of variable ϕ
S_p, S_c = coefficients of linearized source term
T = temperature
u, v = velocities in the axial and radial directions
V = volume
w = tangential velocity due to swirl
W_i = molecular weight of i-species
x, r = coordinates in the axial and radial directions
Y_i = mass fraction of i-species

International Journal of Numerical Methods for Heat & Fluid Flow, Vol. 9 No. 7, 1999, pp. 764-787.

Γ_ϕ	= transport coefficient of variable ϕ	ρ	= fluid density
		ϕ	= transport variable
ε	= dissipation rate of turbulence kinetic energy	ω	= reaction rate
θ_s	= swirling angle	*Subscripts*	
θ_v	= V-gutter flameholder angle	a	= state of air at the inlet
μ_e	= effective viscosity	f	= state of fuel at the inlet
μ_l	= laminar viscosity	f_u	= state of fuel
μ_t	= eddy viscosity	in	= inlet property of combustor
ξ	= mass fraction of atomic species	p, n, e, s ,w	= grid points

Introduction

A principal consideration in combustion-chamber design is the control of flame stabilization and flame propagation under variety of operating conditions. The flames of combustors can be stabilized by recirculation zone (Davies and Beer, 1971), which can be produced by fluids flowing around a bluff-body (such as flameholder), swirling imparted or along a discontinuous boundary surface (such as dump wall). A V-gutter flameholder considered here is often utilized in gas turbine combustor for flame stabilization purposes. Swirl is also used extensively in many combustion systems because it can improve flame stabilization as a result of the formation of the central toroidal recirculation zone (CTRZ) and reduces combustor lengths by producing high entrainment rates of the ambient fluid and fast mixing. On the other hand, side-inlet jets play an important role in the enhancement of combustion performance of the combustor by altering the aerodynamics. In the primary zone, additional air provided by side-inlet nozzles inject on the swirl-induced central circulation region, and it serves to increase mixing and combustion efficiency for stoichiometric conditions. The side-inlet flow can also help complete combustion in the secondary region and renders the combustion products to be cooled and evenly mixed in the dilution zone. However, the swirling flow in sudden-expansion dump combustor with flameholder and side-inlet nozzles have a few researches in the existing literature. The present paper focuses on the interaction effects of central V-gutter flameholder and side-inlet jets on the dump combustor swirling flow using two-step combustion model. The combustor configuration of interest here has numerous flow complexities, involving recirculating flows induced by fluids flowing a discontinuous boundary and bluff-body, flame spreading, turbulent mixing, etc. In order to promote better understanding of the aforementioned complicated flowfield, the numerical simulation of turbulent reacting flows of dump combustor with flameholder and side-inlet nozzles was performed.

In the past, several analytical approaches for solving the combustor flowfield have been attempted. In general, they can be classified by two modeling techniques: "modular" and "unified" models. According to the modular models, the combustor flowfield can be subdivided into separate zones, each of which can be calculated individually, and then all are coupled together to obtain an overall description of the flowfield. A number of examples

of the modular model are available in the literature, such as Swithenback *et al.* (1973), Edelman *et al.* (1980), Harsha and Edelman (1982), and Viets and Drewry (1981). Basically, these reports represent the corner recirculation zone behind the step with a well-stirred reactor model and the core flow with the parabolic form of the governing equations. These two regions are then coupled together with a shear layer model to complete the computational analogy of the combustor flow. However, applications of the modular model are limited since using the model requires a prior knowledge of the flowfield considered. The limitations of the modular approach have lead to the development of the unified approach. The entire flowfield was computed as a unit in the unified approach. There are many literature reports of combustor flow studied by using the "unified" approach. Elghobashi *et al.* (1977) numerically simulated the turbulent mixing of two steady, coaxial jets of equal fluid density in a circular concentric duct with emphasis on studying the concentration fluctuations of species. Hutchinson *et al.* (1977) successfully solved the elliptic form of the governing equations describing the recirculating flow with reaction. The distributions of velocity, temperature and concentration at the combustor outlet when side-inlet jet was introduced into the swirling flowfield were calculated and studied by Serag-Eldin and Spalding (1979) and Shyy *et al.* (1986). Habib and Whitelaw (1980) predicted flowfields for coaxial jets exhausting into a sudden expanding confinement with either the outer or central jet swirling. They observed a large discrepancy between their analytical and experimental results. The discrepancy was attributed to the presence of strong streamline curvatures that were not accounted in their analysis. A similar conclusion was also reached by Srinivasan and Mongia (1980), who predicted the flow in a cold model combustor with a confinement equivalent in diameter to the outer jet diameter. Vanka *et al.* (1983) investigated analytically the flow field characteristics of side-inlet dump combustor by varying the position of dome plate and the angle of side-inlet. They found an optimal head height for the best combustion efficiency. The reacting flow in an axisymmtric combustor with annular side-inlet was investigated by Chen and Tao (1984). Drummond (1985) used the algebraic eddy-viscosity turbulent model and unsplit finite difference technique of MacCormack to study a ramjet dump combustor flowfield. He concluded that the more diffusive than observed in experiments and the over-prediction of the mixing rate is due to the turbulence model adopted. The flow structures, fuel dispersal patterns and temperature field were calculated for a ducted rocket configuration with two side-inlet by Vanka *et al.* (1985) using a one-step combustion model. Lee (1986) numerically investigated nonreacting hydrogen-air mixing in coaxial jets by using one-equation turbulent model and the results agreed well with experimental data. The effect of wall injection flow on the size and shape of the swirling-induced central recirculation zone was investigated by Kilik and Schmidt (1986).

The experimental work is concerned with dump combustor investigation as shown in the literature. Schadow and Chieze (1981) investigated the ignition and combustion problems for ducted rockets using various fuel-rich solid

samples and they concluded that to achieve high combustion efficiency, the requirement of the near-stoichiometric ratio and the gas-phase combustion in the flow region must be satisified. Stull *et al.* (1985) conducted a series of flow-visualization studies to characterize the isothermal combustor flowfield. The velocity and temperature fields in a dilute swirl combustor with jet injection were reported by Rudoff and Samuelson (1986). Liou and Wu (1988) performed detailed mean velocity and turbulence intensity measurements in curved 60-degree inlet ducts and in a three-dimensional side-dump cylindrical combustor using Laser-Doppler velocimetry (LDV).

Dump combustors have been studied extensively because of their ability to burn fuel and contain heat flux in a relatively compact space. Acoustically excited combustion processes are generated in pulse combustor systems (Keller *et al.*, 1994; Barr and Keller; 1994). Pont *et al.* (1998) have studied the emissions reduction and Pyrolysis gas destruction in an acoustically driven dump combustor.

Previous works on the simulation of combustor flowfields used the stream function-vorticity method and the k-ε two-equation turbulence model to analyze a two-dimensional combustor (1979). There have also been studies of combustor flow using p-u-v primitive variables and the k-ε turbulence model (1982). The process incorporated the SIMPLE algorithm technique initiated by Patankar (1980). The SIMPLE-C algorthm developed by Van Doormaal and Raithby (1984) and Latimer and Pollard (1985) has a better convergence rate of residual mass (Hong and Ko, 1987) than that of the SIMPLE algorithm. However, the above studies were limited to reacting flow in a dump combustor with side-inlet or flameholder and did not consider the effects of the interaction between them. The objective here is to investigate the phenomena of reacting flow in a dump combustor with V-gutter flameholder and side-inlet. This paper adopted SIMPLE-C algorithm and turbulence k-ε model to study the interation effects in dump combustor with side-inlet and V-gutter. The finite difference equations are derived by integrating the governing equations over a control volume surrounding each grid point. The power-law scheme (Patankar, 1980) is used for the representation of the convective and diffusive terms across the control surface.

Analytic study

The swirling flow analysis in a sudden-expansion dump combustor with central V-gutter flameholder and side-inlet is very complicated. In order to simplify the problem, the following assumptions are made:

- The flow is two-dimensional axisymmetric and steady state.
- The flow field is composed of a single-phase gaseous flow, i.e. we do not consider a two-phase flow problem.
- The wall thickness of the V-gutter is infinitely thin; the wall of combustor is adiabatic.
- The chemical reaction is two-step and has a finitely fast reaction rate.
- The Lewis number is equal to unity, i.e. there is a linear relation between concentration and total enthalpy of species.

- Both the specific heat at constant pressure and the exchange coefficient are constant.
- The effect of density fluctuations is negligible.
- The effects of radiation and gravity are negligible.

Governing equations

For steady axisymmetric turbulent flow, the general conservative form in cylindrical polar coordinate can be written as

$$\underbrace{\frac{1}{\mathrm{r}}\left[\frac{\partial}{\partial \mathrm{X}}(\rho \mathrm{ur}\phi)+\frac{\partial}{\partial \mathrm{r}}(\rho v \mathrm{r}\phi)\right.}_{\text{convection term}}\underbrace{\left.-\frac{\partial}{\partial \mathrm{X}}(\mathrm{r}\Gamma_{\phi}\frac{\partial \phi}{\partial \mathrm{X}})-\frac{\partial}{\partial \mathrm{r}}(\mathrm{r}\Gamma_{\phi}\frac{\partial \phi}{\partial \mathrm{r}})\right]}_{\text{diffusion term}}=\mathrm{S}^{\phi} \qquad (1)$$

where ϕ stands for the dependent variables (u, v, w, k, ϵ, H, f, $\bar{\mathrm{Y}}_{\mathrm{fu}}$, $\bar{\mathrm{Y}}_{\mathrm{CO}}$), Γ_{ϕ} is the appropriate effective exchange coefficient for the turbulent flow and S^{ϕ} is the source term of the transport equation for ϕ, as shown in Table I.

Turbulence model

The Jones-Launder k-ε two-equation turbulent model was employed in the present study since this model would lead to satisfactory predictions for axisymmetric flow in sudden-expansion dump combustor. The k-ε turbulence model adopts the isotropic viscosity hypothesis and the turbulent viscosity (μ_t) may be related to the turbulent kinetic energy (k) and its dissipation rate (ε) by dimensional analysis

$$\mu_{\mathrm{t}}=\frac{\mathrm{C}_{\mu}\rho \mathrm{k}^2}{\varepsilon} \qquad (2)$$

where $\mathrm{C}_{\mu}=0.09$ is a constant of the model, k and ε are defined as

$$\mathrm{k}=\frac{1}{2}\overline{\mathrm{u}_{\mathrm{i}}^{/}\,\mathrm{u}_{\mathrm{i}}^{/}} \qquad (3)$$

Φ	Γ_{ϕ}	S^{ϕ}							
u	μ_e	$-\frac{\partial P}{\partial x}+\frac{\partial}{\partial x}\left(\mu_e\frac{\partial u}{\partial x}\right)+\frac{1}{r}\frac{\partial}{\partial r}\left(r\mu_e\frac{\partial v}{\partial x}\right)$							
v	μ_e	$-\frac{\partial P}{\partial r}-\frac{2\mu_e\nu}{r^2}+\frac{\rho w^2}{r}+\frac{\partial}{\partial x}\left(\mu_e\frac{\partial u}{\partial r}\right)+\frac{1}{r}\frac{\partial}{\partial r}\left(r\mu_e\frac{\partial v}{\partial r}\right)$							
w	μ_e	$-\frac{\rho v w}{r}-\frac{w}{r^2}\frac{\partial(r,\mu_e)}{\partial r}$							
k	μ_e/σ_k	$\mu\left\{2\left[\left(\frac{\partial u}{\partial x}\right)^2+\left(\frac{\partial v}{\partial r}\right)^2+\left(\frac{\nu}{r}\right)^2\right]+\left[r\frac{\partial}{\partial r}\left(\frac{w}{r}\right)\right]^2+\left(\frac{\partial u}{\partial r}+\frac{\partial v}{\partial x}\right)^2+\left(\frac{\partial w}{\partial x}\right)^2\right\}-\rho\varepsilon$							
ε	μ_e/σ_ε	$\frac{C_1\varepsilon G-C_2\rho\varepsilon^2}{k}$							
f	μ_e/σ_f	0							
H	μ_e/σ_h	0							
m_{fu}	μ_e/σ_{fu}	$\dot{\omega}_{fu}=-\min(R_{kin},R_{ebu})$							
m_{co}	μ_e/σ_{co}	$\dot{\omega}_{co}=-\gamma_2\dot{\omega}_{fu}-(R_{kin},R_{ebu})$							
C_1	C_2	C_{μ}	σ_k	σ_ε	σ_f	σ_h	σ_{fu}	σ_{co}	
1.42	1.92	0.09	1.0	1.3	0.9	0.7	1.0	1.0	

Table I.
Governing equation variables

$$\varepsilon = \frac{\mu_l}{\rho}\overline{\frac{\partial u_i'}{\partial X_j}\frac{\partial u_i'}{\partial X_j}} \tag{4}$$

where μ_l is the laminar viscosity.

The local values of k and ε are determined by their transport partial differential equations in steady state situation as following.

$$\frac{\partial}{\partial X}(\rho uk) + \frac{1}{r}\frac{\partial}{\partial r}(\rho vrk) - \frac{\partial}{\partial X}\left(\frac{\mu_e}{\sigma_k}\frac{\partial k}{\partial X}\right) - \frac{1}{r}\frac{\partial}{\partial r}\left(r\frac{\mu_e}{\sigma_k}\frac{\partial k}{\partial r}\right) = G - \rho\varepsilon \tag{5}$$

$$\frac{\partial}{\partial X}(\rho u\varepsilon) + \frac{1}{r}\frac{\partial}{\partial r}(\rho v r\varepsilon) - \frac{\partial}{\partial X}\left(\frac{\mu_e}{\sigma_e}\frac{\partial \varepsilon}{\partial X}\right) - \frac{1}{r}\frac{\partial}{\partial r}\left(r\frac{\mu_e}{\sigma_e}\frac{\partial \varepsilon}{\partial r}\right) = \frac{\varepsilon}{k}(C_1 G - C_2\rho\varepsilon) \tag{6}$$

where μ_e is the total effective viscosity of the flow. The total effective viscosity μ_e is

$$\mu_e = \mu_l + \mu_t \tag{7}$$

where $C_1 = 1.44$ and $C_2 = 1.92$ are constants in this model, $\sigma_\kappa = 1.0$ and $\sigma_\epsilon = 1.3$ are turbulent Prandtl numbers for k and ε respectively, G denotes the rate of generation of turbulent kinetic energy and is expressed as

$$G = \mu_t\left\{2\left[\left(\frac{\partial u}{\partial X}\right)^2 + \left(\frac{\partial v}{\partial r}\right)^2 + \left(\frac{v}{r}\right)^2\right] + \left[r\frac{\partial}{\partial r}\left(\frac{w}{r}\right)\right]^2 + \left(\frac{\partial u}{\partial r} + \frac{\partial v}{\partial X}\right)^2 + \left(\frac{\partial w}{\partial X}\right)^2\right\} \tag{8}$$

where μ_t is the eddy viscosity.

Combustion model

The mean reaction rate in the species-mass-fraction equation, as shown in Table I, must be determined to complete the fomulation. The simplest and idealized approach for diffusion flames is to invoke an infinitely fast one-step reaction assumption. The reaction proceeds spontaneously once the fuel and oxidant come into contact. That is, the one-step reaction mechanism assumes that the time scale characteristic of reaction is very short compared with those characteristic of convective and diffusive transports, so the chemical reaction goes to completion as soon as the reactants are mixed. The one-step model has been used by many workers but suffers from the disadvantage that dissociation which is important near stoichiometric conditions and intermediates such as CO and H_2 are not represented. In the present study, a two-step global reaction mechanism (Westbrook and Dryer, 1981) is used to describe the combustion of fuel-rich (A/F = 2.24) gases with air. In the present analysis, C_3H_8 is used as the fuel and thus the chemical reaction mechanism can be written as

$$C_3H_8 + 3.5(O_2 + nN_2) \rightarrow 3CO + 4H_2O + N_2 \tag{9a}$$

$$3CO + 1.5(O_2 + nN_2) \rightarrow 3CO_2 + 1.5nN_2 \tag{9b}$$

According to the conservation of atomic species C, H and O, the three conserved parameters and another conserved scalar, mixture fraction f, are defined as

$$\xi_1 = \left(\frac{W_{CO_2}}{W_C}\right)\xi_C = \bar{Y}_{CO_2} + \gamma_5\bar{Y}_{CO} + \gamma_2\gamma_5\bar{Y}_{fu} \tag{10a}$$

$$\xi_2 = \frac{1}{2}\left(\frac{W_{H_2O}}{W_H}\right)\xi_H = \overline{Y}_{H_2O} + \gamma_3\overline{Y}_{fu} \tag{10b}$$

$$\begin{aligned}\xi_3 =& \frac{1}{2}\left(\frac{W_{O_2}}{W_O}\right)\xi_O - \left(\frac{W_{O_2}}{W_{CO_2}}\right)\xi_1 - \frac{1}{2}\left(\frac{W_{O_2}}{W_{H_2O}}\right)\xi_2 \\ =& \overline{Y}_{O_2} - (\gamma_1 + \gamma_2\gamma_4)\overline{Y}_{fu} - \gamma_4\overline{Y}_{CO}\end{aligned} \tag{10c}$$

$$f = \frac{\xi_n - \xi_{n,a}}{\xi_{n,f} - \xi_{n,a}} \tag{11}$$

where

$$\gamma_1 = \frac{3.5W_{O_2}}{W_{fu}}$$

$$\gamma_2 = \frac{3W_{CO}}{W_{fu}}$$

$$\gamma_3 = \frac{4W_{H_2O}}{W_{fu}}$$

$$\gamma_4 = \frac{0.5W_{O_2}}{W_{CO}}$$

$$\gamma_5 = \frac{W_{CO_2}}{W_{CO}}$$

The variables ξ_C, ξ_H and ξ_O represent the mass fractions of atomic species C, H and O respectively, ξ_n stands for any conserved parameter which is not affected by sources and sinks, W_i and $\overline{Y}_i$ represent the molecular weight and mass fraction of i-species respectively, and subscripts a and f denote the state of air and fuel at the inlet respectively. Substituting equation (10) into equation (11) and rearranging the result, we can obtain three relations for the mass fraction of O_2, H_2O and CO_2 in terms of those of fuel (i.e. C_3H_8) and CO, and the mixture fraction f

$$\overline{Y}_{O_2} = (1 - f)\overline{Y}_{O_2,a} - (f\overline{Y}_{fu,f} - \overline{Y}_{fu})(\gamma_1 + \gamma_2\gamma_4) + \gamma_4\overline{Y}_{CO} \tag{12a}$$

$$\overline{Y}_{H_2O} = \gamma_3(f\overline{Y}_{fu,f} - \overline{Y}_{fu}) + f\overline{Y}_{H_2O,f} \tag{12b}$$

$$\overline{Y}_{CO_2} = \gamma_2\gamma_5(f\overline{Y}_{fu,f} - \overline{Y}_{fu}) - \gamma_5\overline{Y}_{CO} + f\overline{Y}_{CO_2,f} \tag{12c}$$

The conservation of mass leads to the expression for the mass fraction of N_2

$$\overline{Y}_{N_2} = 1 - \overline{Y}_{fu} - \overline{Y}_{O_2} - \overline{Y}_{CO} - \overline{Y}_{H_2O} - \overline{Y}_{CO_2} \tag{12d}$$

The present combustor reacting flowfield calculated with central V-gutter

flameholder and side-inlet flow is very complex, so for the combustion processes the effect of the comparison between turbulent mixing and chemical kinetic must be considered. The eddy-breakup rate is compared with the Arrhenius type rate of reaction, and the smaller of the two rates controls the reaction rate. Therefore, the mean reaction rates $\dot{\omega}_{fu}$ and $\dot{\omega}_{CO}$ in the species equation can be determined as follows:

$$\dot{\omega}_{fu} = -\min \begin{cases} A_1 \rho^{1.5} \overline{Y}_{fu}^{0.5} \overline{Y}_{O_2} \exp\left(\frac{-E_1}{R_u T}\right) \\ C_{R1} \rho \min\left[\overline{Y}_{fu}, \frac{\overline{Y}_{O_2}}{\gamma_1}\right] \frac{\varepsilon}{\kappa} \end{cases} \tag{13a}$$

$$\dot{\omega}_{co} = -\gamma_2 \dot{\omega}_{fu} - \min \begin{cases} A_2 \rho^2 \overline{Y}_{co} \overline{Y}_{O_2} \exp\left(\frac{-E_1}{R_u T}\right) \\ C_{R2} \rho \min\left[\overline{Y}_{CO}, \frac{\overline{Y}_{O_2}}{\gamma_4}\right] \frac{\varepsilon}{\kappa} \end{cases} \tag{13b}$$

where

$A = 3.3 \times 10^{14}$

$A_2 = 6.0 \times 10^8$

$\frac{E_1}{R_u} = 27,000$

$\frac{E_2}{R_u} = 12{,}500$

$C_{R1} = 3.0$

$C_{R2} = 4.0$

Numerical method

Grids system and irregular boundary

The staggered grid (Patankar, 1980) arrangement of integration over control volume was used to avoid the wavy phenomena, as shown in Figure 1. The nodes of the velocity grid were located midway between the scalar grid nodes to present the true convective quantities across the boundary of control volume. After checking the grid independence and convergence rate, as shown in Figures 2-3, the calculations were made using a 58 × 31 grid system for both cold and reaction flow. The arrangement of grid system and the irregular boundary of ladder-type V-gutter are shown in Figure 4. The grid size contracts in the radial direction and expands in the axial direction from the sudden expansion towards downstream; hence a finer grid spacing is formed near the combustor wall and the vertical wall at the sudden expansion respectively. In the present computation domain a 58 × 31 grid system with 0.95 contraction in the radial direction and 1.05 expansion in the axial direction is employed. The central processor time on a CDC Cyber 180/380 computer is about 6h to convergence for 300 iterations per case. The convergence conditions are local residual less than or equal to 10^{-6} and total residual less than or equal to 10^{-4}.

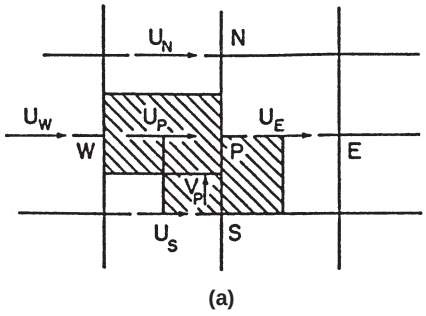

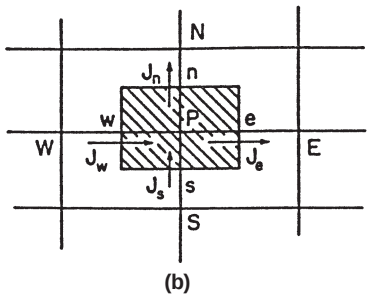

Figure 1.
Control volumes and staggered grid arrangement (a) for variables u, v; (b) fo other variable ϕ except u, v

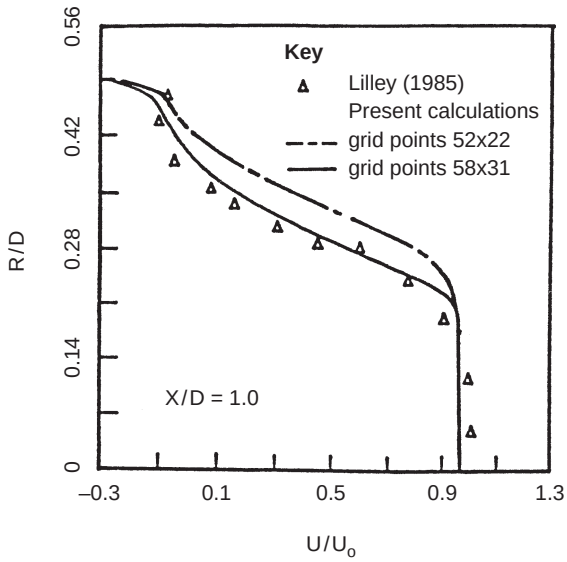

Figure 2.
Axial velocity distribution of dump combustor ($\theta = 0^o$, X/D = 1)

Finite difference equations

Integration over the control volume cell was employed to construct the finite difference equations. First, the general form of equation (1) can be written as

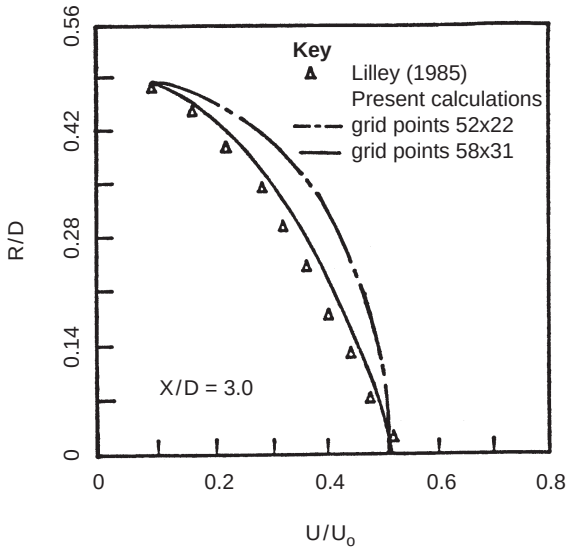

Figure 3.
Axial velocity distribution of dump combustor ($\theta = 0^o$, X/D =3)

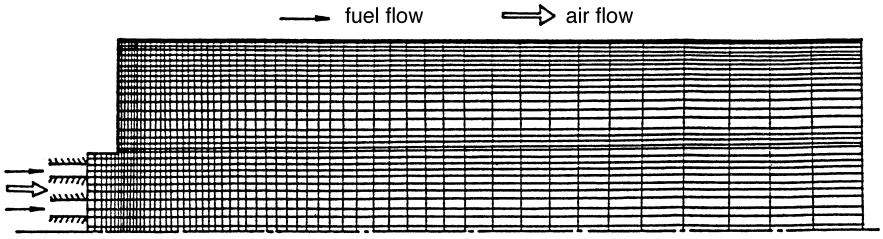

Figure 4.
Spacing of grids and ladder-type arrangement of V-gutter

$$\frac{\partial(\rho\phi)}{\partial t} + \frac{\partial J_x}{\partial x} + \frac{\partial J_y}{\partial y} = S, \tag{14}$$

where

$$J_x = \rho u\phi - \Gamma\frac{\partial\phi}{\partial x}, \qquad J_y = \rho v\phi - \Gamma\frac{\partial\phi}{\partial y},$$

Integration of equation (14) over the control volume gives

$$\iiint_{\mathrm{v}} \left(\frac{\partial(\phi)}{\partial \mathrm{t}} + \frac{\partial \mathrm{J_x}}{\partial \mathrm{x}} + \frac{\partial \mathrm{J_y}}{\partial \mathrm{y}}\right) \mathrm{dV} = \iiint_{\mathrm{v}} \mathrm{SdV}, \tag{15}$$

where $dV = dxdydz = dxdy$. The finite difference equation for equation (15) with linearized source term is

$$\frac{(\rho_p\phi_p - \rho_p^o\phi_p^o)\Delta x\Delta y}{\Delta t} + J_e - J_w + J_n - J_s = (S_p\phi_p + S_c)\Delta x\Delta y \tag{16}$$

where

$$J_i = \int J_x dy|_{\text{over interface i}} \ (i = E, W), \quad J_i = \int J_y dx|_{\text{over interface i}} \ (i = N, S).$$

Also, integration of the continuity equation over the control volume cell gives

$$\frac{(\rho_p - \rho_p^o)}{\Delta t} + F_e - F_w + F_n - F_s = 0 \tag{17}$$

Subtracting equation (17) multiplied by ϕ_p from equation (16) gives

$$\begin{aligned} \rho_P^o(\phi_p - \phi_P^o)\frac{\Delta x \Delta y}{\Delta t} + (J_e - F_e\phi_p) - (J_w - F_w\phi_p) + (J_n - F_n\phi_p) \\ - (J_s - F_s\phi_p) = (S_p\phi_p + S_c)\Delta x \Delta y \end{aligned} \tag{18}$$

where F_i is the mass flow rate for surface i of the control volume. Then the total flux of control volume cell can be written as

$$J_i - F_i\phi_p = a_i(\phi_p - \phi_i) \ \ (i = E, N), \quad J_i - F_i\phi_p = a_i(\phi_i - \phi_p)(i = W, S), \tag{19}$$

where

$$a_i = D_i A(|P_i|) + [-F_i, 0](i = E, N), \quad a_i = D_i A(|P_i|) + [F_i, 0](i = W, S),$$

$P_i = F_i/D_i$ is the Peclet number for surface i, $A(|P_i|)$ is a function of P_i and

$$D_i = \Gamma_i A_i / (\partial x)_i$$

Substituting these relations in equation (18), we obtain

$$a_P\phi_P = a_E\phi_E + a_W\phi_W + a_S\phi_S + a_N\phi_N + b \tag{20}$$

where

$$b = S_c\Delta x\Delta y + a\phi_P^o, \ a_P^o = \rho_P^o\Delta x\Delta y/\Delta t, \ a_P = a_E + a_W + a_S + a_N + a_P^o - S_p\Delta x\Delta y$$

Details of the SIMPLE-C algorithm (Van Doormaal and Raithby, 1984) calculation procedures and the power-law scheme will not be repeated here.

Integration over control volume and power law scheme are employed to construct the finite difference equations. The general forms of finite difference equations for equation (1) with a linearized source term are given as follows.

- Finite difference equation of the axial momentum

$$(a_E - S_p^u)u_E = \sum a_{nb}u_{nb} + S_C^u + (P_p - P_E)A_E \tag{21}$$

- Finite difference equation of the radial momentum

$$(a_N - S_p^u)u_N = \sum a_{nb}u_{nb} + S_C^u + (P_p - P_N)A_N \tag{22}$$

- Finite difference equation of the other variables

$$(a_P - S_p^\phi)\phi_P = \sum a_{nb}\phi_{nb} + S_P^\phi \tag{23}$$

Solution technique

The SIMPLE-C algorithm developed by van Doormaal and Raithby (1984) was employed to solve the present problem. The solution procedure is initiated with guesses for the velocity and pressure fields and then proceeds with line-by-line tridiagonal matrix algorithm (TDMA) method that treats the dependent variables in the x and r directions alternatively. After each sweep over the solution domain, updating velocity, pressure and density fields are made by the correction equation. The corrective pressure equation is according to the SIMPLE-C algorithm (van Doormaal and Raithby, 1984), and the corrective density equation is found by the equation state of gas. The other dependent variables (w, k, ε, H, f, $\overline{Y}_{fu}$, $\overline{Y}_{CO}$) are also solved line-by-line simultaneously with the mean velocity distribution. The procedure is repeated until the continuity equation is satisfied to an allowable normalized mass residual tolerance of 10^{-4}. In order to avoid numerical instability and enhance compulational efficiency, the under-relaxation factor was used in calculation procedure. The under-relaxation factors used in the present calculations are shown in Table II.

Boundary conditions

The above set of finite difference equations has to be solved with following boundary conditions:

(1) At the inlet: uniform velocity (U_{in}), air temperature (T_{in}) and fuel temperature (T_{fu}) are assumed at the combustor inlet.

$$u = U_{in}$$
$$v = 0$$
$$w = U_{in} \tan \theta_s$$
$$P_{fu} = 1{,}013\text{kPa}$$
$$P_{air} = 535\text{kPa}$$
$$T_{fu} = 1{,}000K$$
$$T_{air} = 500K$$
$$\rho_{fu} = P_{fu}/R_{fu}T_{fu}$$
$$\rho_{air} = P_{air}/R_{air}T_{air}$$
$$k_{in} = 0.003U_{in}^2$$
$$\varepsilon_{in} = \frac{C_\mu k_{in}^{\frac{3}{2}}}{(0.03 \times d)}$$

	u	v	w	k	ε	p'	H	f	$Y_f u$	$Y_c o$
Cold flow	0.4	0.4	0.3	0.5	0.3	0.8				
Reacting flow										
One-step	0.3	0.2	0.3	0.2	0.2	0.8	0.2	0.2		
Two-step	0.3	0.2	0.3	0.2	0.3	0.8	0.3	0.3	0.4	0.4

Table II. Under-relaxation factors

$$\overline{Y}_{CO} = 0$$

The inlet velocity of the fuel injection was determined by the air-fuel ratio, and

$$f = 0, \overline{Y}_{fu} = 0, H_{air} = C_P T_{in} + \frac{(u^2 + v^2 + w^2)}{2}$$

in the region of the air inlet,

$$f = 1, \overline{Y}_{fu} = 1, H_{fu} = C_P T_{fu} + \frac{(u^2 + v^2 + w^2)}{2} + \Delta h_f^o$$

in the region of the fuel inlet.

(2) At centerline

$$\nu = 0, w = 0, \frac{\partial \phi}{\partial r} = 0 \qquad (\phi = u, k, \varepsilon, H, f, \overline{Y}_{fu}, \overline{Y}_{CO}$$

(3) At the wall

$$\frac{\partial H}{\partial n} = 0, \phi = 0;$$

close the wall, the k and ε were handled by wall function (Launder and Spalding, 1972).

(4) At the exit

$$v = 0, \frac{\partial \phi}{\partial x} = 0$$

(fully developed flow).

Results and discussion

The study is initially to investigate the effects of central V-gutter flameholder on the swirling flows by using one-step instantaneous chemical reaction model, and subsquently to study how the various species-mass-fraction distribution in the reaction flow were affected by the introduction of six side-inlet flow into the dump-combustor chamber mentioned above by employing two-step combustion model with finite chemical reaction rate. In the present calculations, the configuration of physical plane in cold and reaction flow are shown in Figures 5 and 6 respectively. The simulated combustor condition in cold and reaction flow is shown in Tables III and IV respectively. The calculated results were first checked with the available predictions (Renn and Su, 1985), in which DR = 0.25, BR = 0.25 , and Re = 3.225×10^5. The total pressure coefficient C_{pt} and normalized central axial-velocity U/U_o in cold flow were solved firstly and shown an excellent agreement with the predictions data of Renn and Su (1985), as shown in Figure 7. The calculated results of velocity

field have compared with the experimental data of Lilley (1985) at a swirling angle of 45°, as shown in Figures 8 and 9. It is shown that there is an agreement with the prediction data of Lilley (1985).

The effects of swirl on the velocity field

The axial-velocity of central axial in cold flow with different swirl are shown in Figure 10. From these figures we find that the swirl (i.e. swirl angle $\theta_s = \tan^{-1}\frac{W_{in}}{U_{in}}$) affects the flowfield structure. While the swirl is zero, there is a central recirculation zone (called CTRZ1) induced behind the V-gutter flameholder expect for the corner recirculation zone (called CRZ) behind the combustor dump-step. However, additional central recirculation zone (called CTRZ2) behind CTRZ1 is induced due to the central axial-velocity reduced with

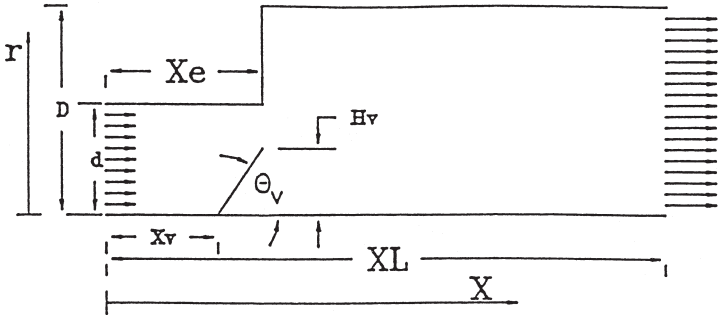

Figure 5.
The configuration 1 of combustor chamber considered

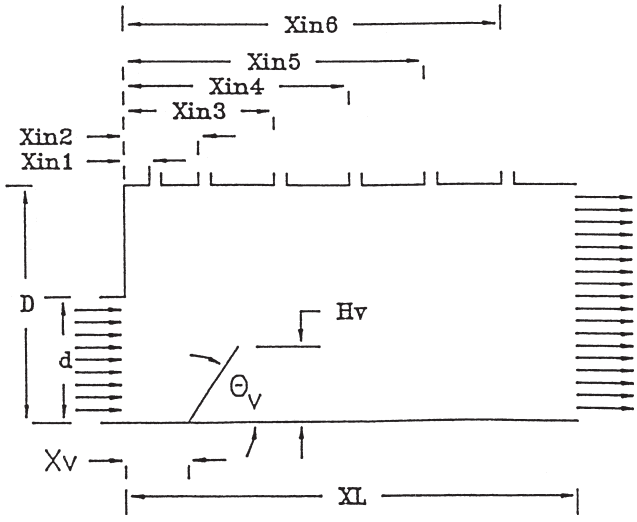

Figure 6.
The configuration 2 of combustor chamber considered

Radius of the combustor, D	= 0.08m					
Radius of the combustor inlet, d	= 0.04m					
Length of the combustor, XL	= 0.8m					
Length of the combustor inlet, Xe	= 0.8m					
Dump ratio, $(D - d)^2/D^2$	0.25, 0.444					
Swirling angle		0°	15°	30°	45°	60°
V-gutter						
Angle	Hv/D	Xv/D				
26.56 ≈ 30°	0.25	0.075				
45°	0.25	0.1				
63.45 ≈ 60°	0.25	0.125				
Re		3.265E+5	4.306E+5		5.382E+5	
Inlet temperature of the combustor	= 300°K					
Inlet pressure of the combustor	= 1atm					

Table III.
Flowfield conditions of the cold flow

Length of the combustor, XL	= 0.8m					
Radius of the combustor, D	= 0.08m					
Radius of the combustor inlet, d	= 0.04m					
Radius of fuel-inlet	= 0.004m					
Position of fuel-inlet (r-dir.)	= 0.016m, 0.032m					
Position of the side inlet, Xin1/XL	= 0.0517					
Xin2/XL	= 0.1379					
Xin3/XL	= 0.3103					
Xin4/XL	= 0.4828					
Xin5/XL	= 0.6552					
Xin6/XL	= 0.8276					
Width of side-inlet nozzle Xa/XL	= 0.01724					
Injection angle of side-inlet	= 90°					
Mass fraction of side-inlet		1%	5%	10%	20%	
Swirling angle	0°	15°	30°	45°	60°	
V-gutter						
Angle		Hv/D			Xv/D	
15°		0.25		0.1293	0.3017	0.4741
30°		0.35		0.1293	0.3017	0.4741
45°	0.3	0.4	0.5	0.1293	0.3017	0.4741
Reyolds number, Re	= 3.665E+5					
Air-fuel ratio, A/F	= 2.24					
Inlet temperature of fuel	= 1,000°K					
Inlet temperature of air	= 500°K					
Inlet pressure of fuel	= 1,013kPa					
Inlet pressure of airl	= 535kPa					
Fuel	= C_3H_8					

Table IV.
Flowfield conditions of the reacting flow

the increasing of centrifugal force when swirl angle is increased , for example swirl angle is 30°. When swirl angle is 45°, before V-gutter flamehold central recirculation zone (called CRTZ3) is generated and concurrently the coupled CRTZ1 and CRTZ2 form a new larger recirculation zone; the result is also because the greater swirl effect causes stronger adverse-flowing around the central axis.

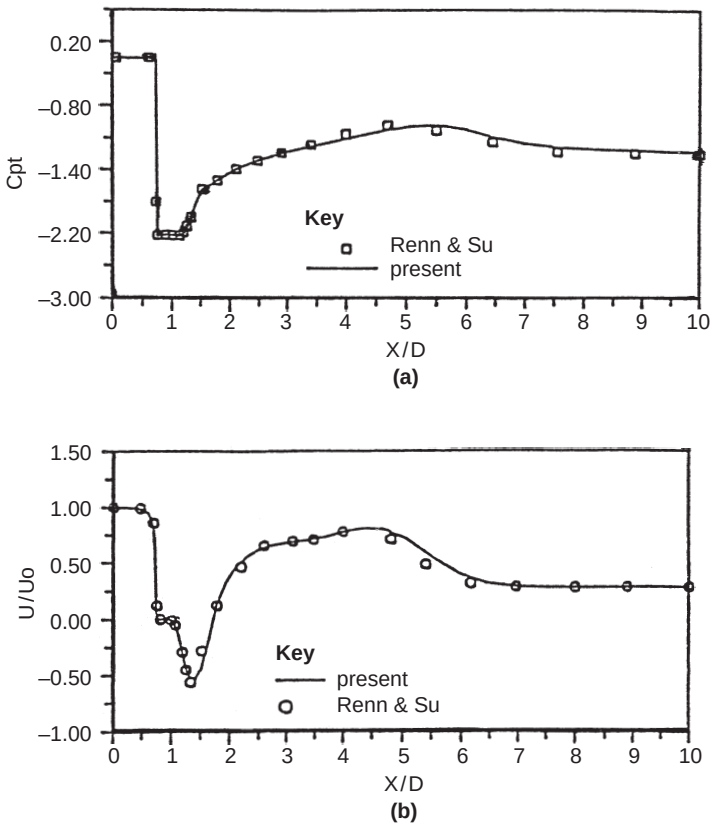

Figure 7.
Comparison of predicted results (a) for C_{pt}; (b) for central axial-velocity

The effects of flameholder angle on the velocity field

At a fixed swirl strength the velocity fields for θ_v =15°, 30° and 45° in reaction flow are shown in Figure 11. From this figure it shows that, as expected, the length of CRTZ becomes shorter with the increasing of θ_v. Typically, the general trend of flow patterns of reaction flow is similar to that of cold flow, but in reaction flow there are smaller CRZ and CRTZ as well as greater axial-velocity at the combustor outlet; the result is because the released chemical reaction heat of combustion causes the increasing of kinetic energy throughout the overall combustor flowfield, as shown in Figure 11.

The predicted species-mass-fraction distribution

Qualitatively, two-step chemical reaction mechanism enough described the physical phenomena of combustor flowfield, but the intermediates such as CO and N_2 must be considered when precise predictions are desired quantatively. Furthermore, based on the knowledge of production distribution of H_2O, CO_2, CO, O_2, N_2 the occurring position of mixing flame can be estimated and it is very useful for the design of combustor configuration and materials used. Based on above consideration, in the current study the species-mass-fraction

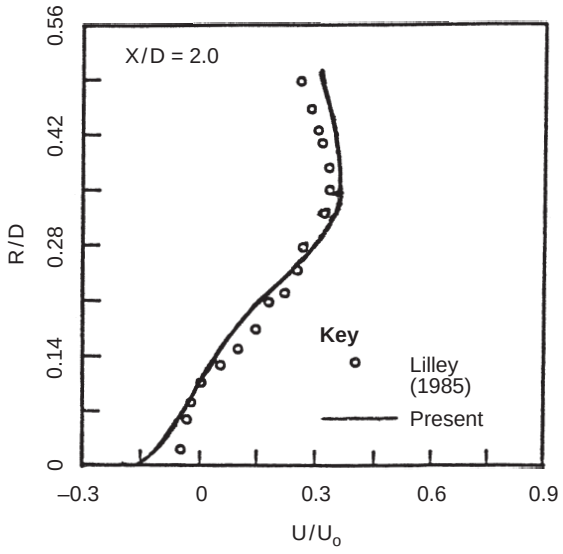

Figure 8.
Axial velocity distribution (θ = 45°)

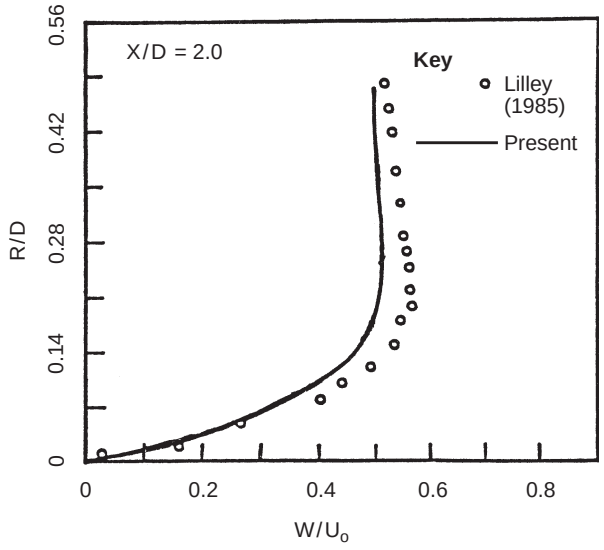

Figure 9.
Tangential velocity distribution (θ = 45°)

distribution are investigated using two-step combustion model with finite chemical reaction rate.

Figure 12 shows the temperature distribution for θ_v = 45°, θ_S = 0°, X_V/D = 0.3017 and H_ν/D = 0.4 in reaction flow. We find that maximum temperature is around 2,000°K at the front of V-gutter flameholder and corner recirculation zone. This is due to the existence of blockage of flameholder causes better mixing effect at the front of V-gutter and concurrently renders the high-temperature

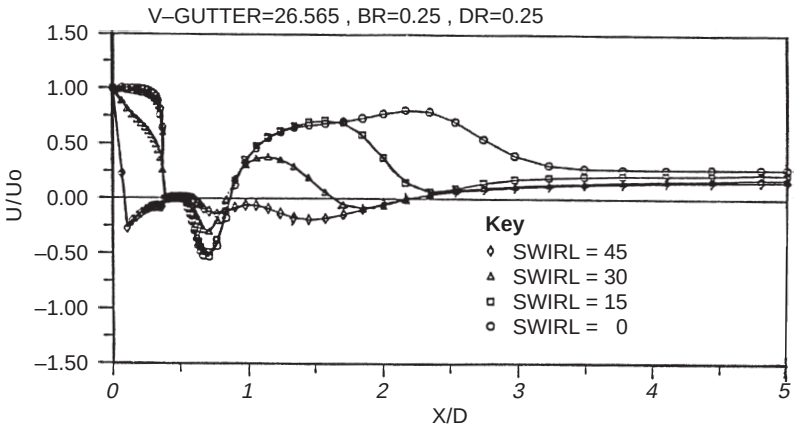

Figure 10.
The axial velocity of central axis at different swirl angles

fluids to be directed toward the solid walls behind the combustor dump-step, as shown in Figure 12. The temperature near six side-inlet nozzles are obviously smaller since the fluids injected are standard atmospheric air. The distribution of species-mass-fraction of fuel, H_2O, CO_2, CO, O_2, N_2 are shown in Figures 13-18 respectively. The recirculation zone behind V-gutter is a low velocity region, so the fuel recirculated at the inner-side region of V-gutter; the fuel distribution is lower around the corner recirculation zone since the most violent combustion/chemical reaction occurs at this region to exhaust more fuel, as shown in Figure 13.

From the equation (13b) it indicates that the production rate of CO depends on the distribution of fuel and O_2 ; the amount of intermediate CO increases with combustion rate, because the increased amount of fuel causes more effective mixing rate. Similarly, the distribution of CO similar to that of fuel is more intensive at the inner-side region of V-gutter, as shown in Figure 14. In the Figure 14 the distribution amount of CO is more around the six side-inlet since the air injected by these jets will react with the fuel. Both CO_2 and H_2O are the products after chemical/combustion reaction; with the increasing of temperature the chemical reaction will accelerate accordingly, so the distributions of CO_2 and H_2O are related to reaction temperature. The general distribution of CO_2 and H_2O is similar to that of temperature as shown in Figures 15 and 16, respectively. From Figure 17 it indicates that behind the V-gutter the mass-fraction of O_2 is almost zero.

The result is due to the fact that the prescribed inlet condition is rich-fuel (A/F = 2.24) to exhaust the O_2 quickly. N_2 is the only species that does not join in chemical/combustion reaction, so the distribution of N_2 only depends on the flowing conditions of combustor. Figure 18 indicates that N_2 injected from combustor inlet directs toward the solid walls due to the blockage of central V-gutter flameholder.

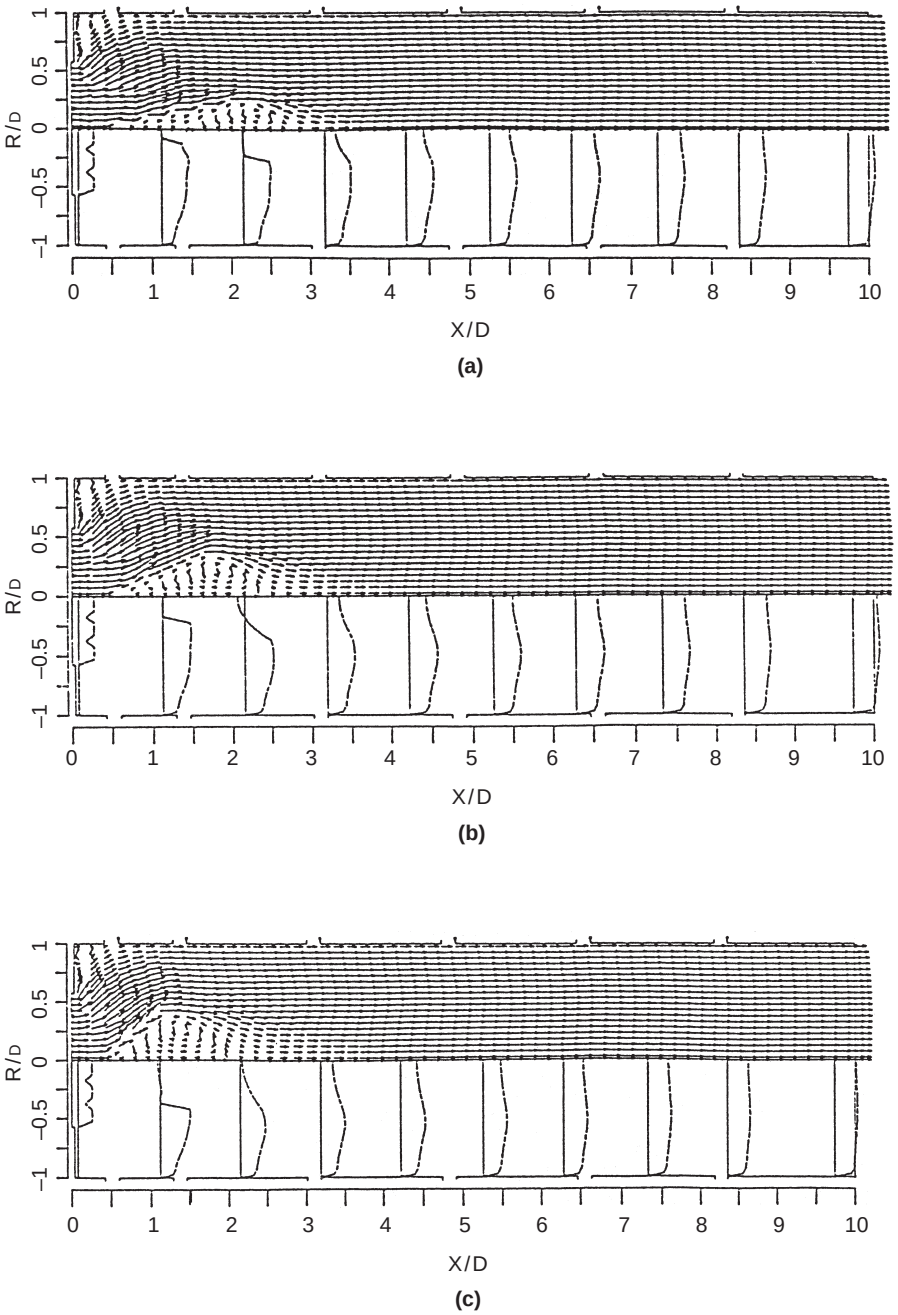

Figure 11.
The velocity vectors and profiles at different V-gutter angle (a) for θ_v = 15°; (b) for θ_v = 30°; (c) for θ_v = 45°

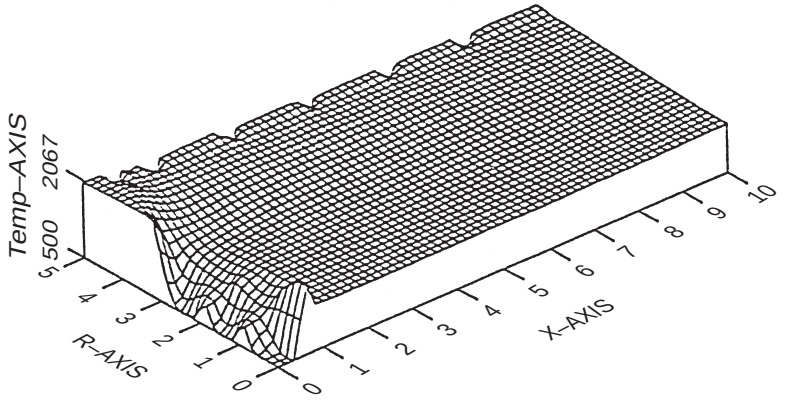

Figure 12.
Temperature distributions for θ_v = 45°, θ_s = 0°, X_v/D = 0.3017 and h_v/D = 0.4

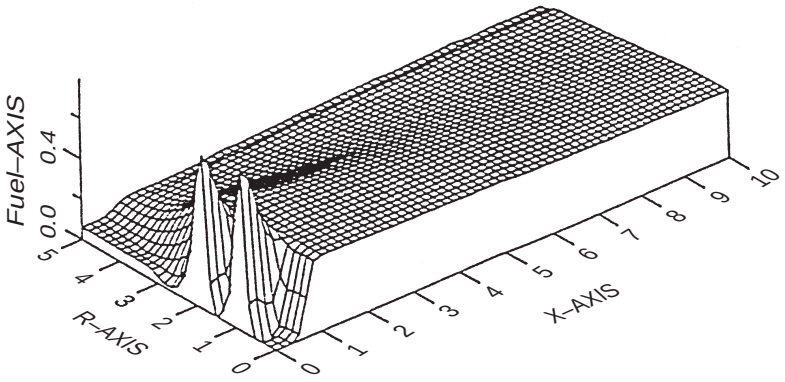

Figure 13.
The distribution of mass-fraction of fuel

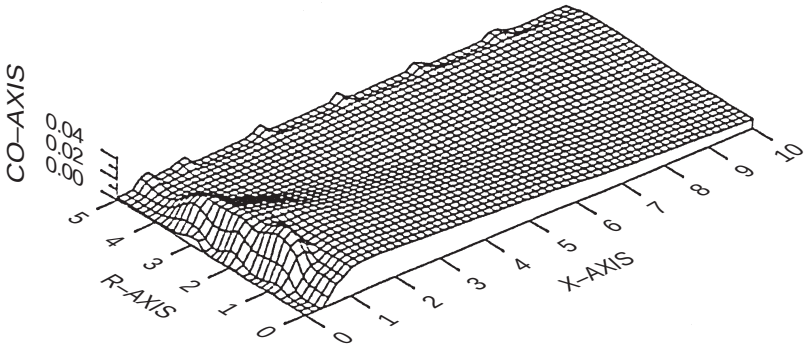

Figure 14.
The distribution of mass-fraction of CO

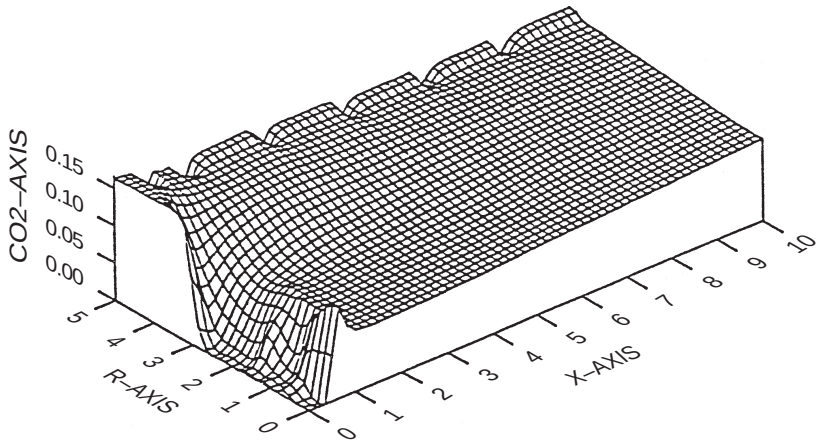

Figure 15.
The distribution of mass-fraction CO_2

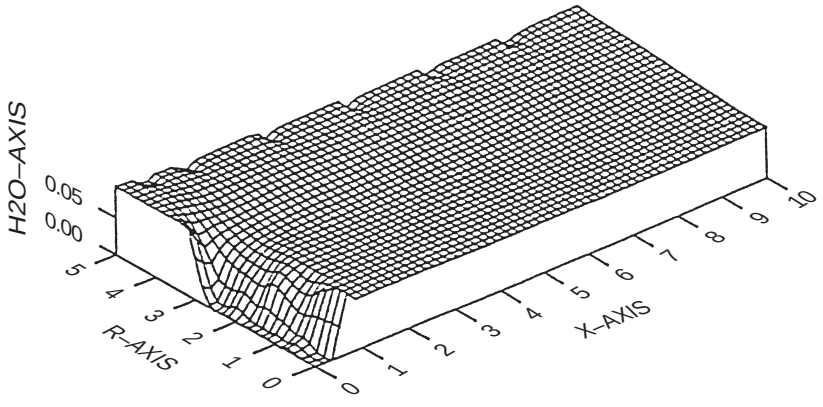

Figure 16.
The distribution of mass-fraction of H_2O

Concluding remarks

Numerical simulation of the swirling flow of dump combustor with central V-gutter flameholder and six side-inlet are calculated in the present paper. From the above discussion and analysis, it may be concluded that:

- The flowfield structure of combustor considered is strongly affected by the swirl and flameholder.
- The length of central recirculation zone is decreased when the angle of V-gutter flameholder is incresased for the fixed strength of swirl.
- The corner recirculation zone and central recirculation zone in reacting flow become smaller than those in cold flow because released heat of combustion causes the increase of kinetic energy throughout the overall combustor flowfield.

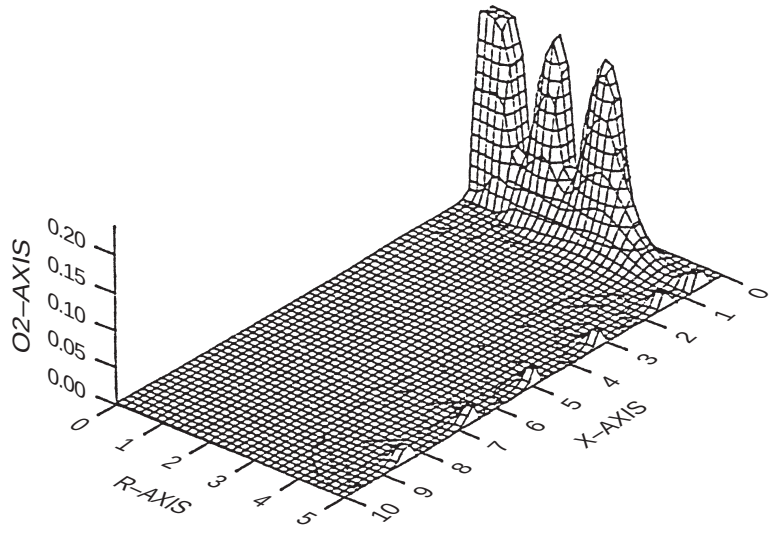

Figure 17.
The distribution of mass-fraction of O_2

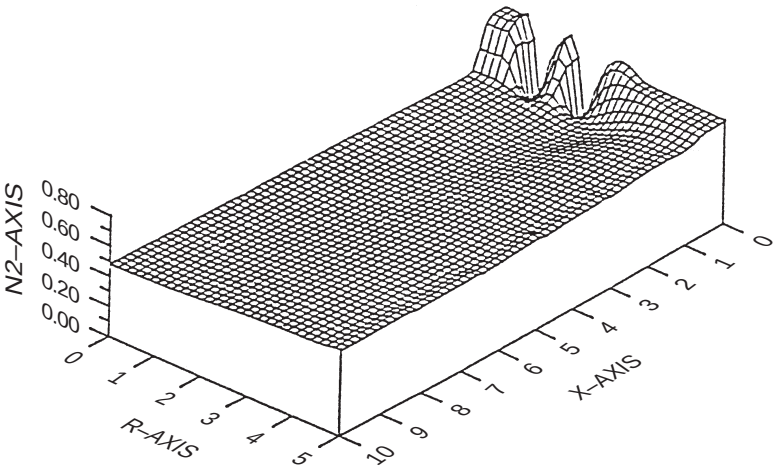

Figure 18.
The distribution of mass-fraction of N_2

- In reacting flow of dump combustor with flameholder the maximum temperature is at the front of V-gutter and corner recirculation zone.
- The distribution of fuel is lower around the corner recirculation zone since most violent combustion/chemical reaction occurs at this region.
- The distribution of CO_2 and H_2O is similar to that of temperature since the production rate of CO_2 and H_2O strongly depends on the temperature.

References

Barr, P.K. and Keller, J.O. (1994), "Premixed combustion in a periodic flow field. Part II: importance of flame extinction by fluid dynamic strain", *Combust. & Flame*, Vol. 99, pp. 43-52.

Chen, L. and Tao, C.C. (1984), *Study of the Side-inlet Dump combustor of Solid-ducted Rocket with Reacting Flow*, AIAA paper 84-1378.

Davies, T.W. and Beer, J.M. (1971), "Flow in the wake of bluff-body flame dtabilizer", *13th Symp. (Int.) on Combustion*, pp. 631-8.

Drummond, J.P. (1985), "Numerical study of a ramjet dump combustor flowfield", *AIAA J.*, Vol. 23 No. 4, pp. 604-11.

Edelman, R.B., Harsha, P.T. and Schmotolocha, S. (1980), *Modelling Techniques for the Analysis of Ramjet Combustion Proccesses*, AIAA paper 80-1190.

Elghobashi, S.H., Pun, W.M. and Spalding, D.B. (1977), "Concentration fluctuation in isothermal turbulent confined coaxial jets", *Chemical Engineering Science*, Vol. 32, pp. 161-6.

Habib, M.A. and Whitelaw, J.H. (1980), "Velocity characteristic of confined co-axial jets with and without swirl", *Transactions of ASME, J. of Fluids Engineering*, Vol. 102, pp. 47-53.

Harsha, P.T. and Edelman, R.B. (1982), "Assessment of modular ramjet combustor model", *J. of Spacecraft*, Vol. 19, pp. 430-36.

Hong, Z.C. and Ko, T.K. (1987), "A study on the flow field in a 3D side-inlet dump combustor with different side-inlet angles", *The Natl. Conf. On Theoretical and Applied Mechanics, Taipei*, pp. 211-23.

Hutchinson, P., Khalil, E.E. and Whitelaw, J.H. (1977), "Measurement and calculation of furnace-flow properties", *J. of Energy*, Vol. 1, pp. 212-19.

Keller, J.O., Barr, P.K. and Gemmen, R.S. (1994), " Premixed combustion in a periodic flow field. Part I: experimental investigation", *Combust. & Flame*, Vol. 99, pp. 29-42.

Kilik, E. and Schmidt, P. (1986), *A Numerical Study of Coaxial Swirl Flow with Wall Mass Injection*, AIAA paper 86-0369.

Latimer, B.R. and Pollard, A. (1985), "Comparison of pressure-velocity coupling solution algorithm", *Numer. Heat Transfer*, Vol. 8, pp. 635-52.

Launder, B.E. and Spalding, D.B. (1972), *Lectures on Mathematical Model of Turbulence*, Academic Press, London.

Lee, S.C. (1986), "Turbulent mixing of coaxial jets between hydrogen and air", *Int. J. Hydrogen Energy*, Vol. 11 No. 12, pp. 807-16.

Lilley, D.G. (1985), *Investigations of Flow Fields Found in Typical Combustor Geometrics*, NASA CR-3869.

Liou, T.M. and Wu, S.M. (1988), "Flow field in a dual-inlet side-dump combustor", *J. of Propulsion and Power*, Vol. 4 No. 1, pp. 53-60.

Patankar, S.V. (1980), *Numerical Heat Transfer and Fluid Flow*, Hemisphere, New York, NY.

Pont, G., Cadou, C.P., Karagozian, A.R. and Smith, O.I. (1998), "Emissions reduction and pyroolysis gas destruction in an acoustically driven dump combustor", *Combust. and Flame*, Vol. 113, pp. 249-57.

Renn, G.D. and Su, Y.B. (1985), "Numerical simulation in sudden-expansion dump combustor with flameholder", *Trans. of AASRC*, pp. 13-24.

Rudoff, R.C. and Samuelsen, G.S. (1986), *Detailed Measurements of Velicity, Temperature, and Soot in a Model Gas Turbine Combustor with Wall Injection*, AIAA paper 86-0523.

Schadow, K.C. and Chieze, D.J. (1981), "Water tunnel and windowed combustion as tools for ducted rocket development", *Proceedings of 1981 JANNAF Propulsion Meeting*, CPIA Pub. 340, Vol. 2, pp. 101-15.

Serag-Eldin, M.A. and Spalding, D.B. (1979), "Computations of three-dimensional gas turbine combustion chamber flows", *ASME Journal of Engineering for Power*, Vol. 101, pp. 326-36.

Shyy, W., Braaten M.E. and Correa, S.M. (1986), *A Numerical Study of Flow in a Combustor with Dilution Holes*, AIAA paper 86-0057.

Srinivasan, R. and Mongia, H.C. (1980), *Numerical Computation of Swirling Recirculating Flow, Final Report*, NASA CR-165196.

Stull, F.D., Craig, R.R., Streby, G.D. and Vanka, S.P. (1985), "Investigation of a dual inlet side dump combustor using liquid fuel injection", *J. of Propulsion and Power*, Vol. 1, pp. 83-8.

Swithenback, J., Poll, I., Vincent, M.W. and Wright, D.D. (1973), "Combustion design fundamentals", *14th Symp. (Int.) on Combustion*, pp. 627-36.

Van Doormaal, J.P. and Raithby, G.D. (1984), "Enhancements of the SIMPLE method for predicting incompressible fluid flows", *Number. Heat Transfer*, Vol. 7, pp. 147-63.

Vanka, S.P., Craig, R.R. and Stull, F.D. (1985), *Mixing, Chemical Reaction and Flow Field Development in Ducted Rockets*, AIAA paper 85-1271.

Vanka, S.P., Stull, F.D. and Craig, R.R. (1983), *Analytical Characterization of Flow Field in Side Inlet Dump Combustor*, AIAA paper 83-1399.

Viets, H. and Drewry, J.E. (1981), "Quantitative predictions of dump combustor flow field", *AIAA J.*, Vol. 19 No. 4, pp. 484-91.

Westbrook, C.K. and Dryer, F.C. (1981), "Simplified reaction mechanisms for the oxidation of hydrocarbon fuels in flames", *Combustion of Science and Technology*, Vol. 27, pp. 31-43.

Further reading

Lilley, D.B. (1979), "Flowfield modeling in practical combustor: a review", *J. of Energy*, Vol. 3, pp. 193-210.

Vatistas, G.H., Lin, S., Kwok, C.K. and Lilley. D.G. (1982), *Bluff-body Flameholder Wakes: A Simple Numerical Solution*, AIAA paper 82-1177.